Sclareol purification using the supercritical fractionation process: A modeling case study

C. Dufour, Christelle Crampon, C. Delbecque, P-P. Garry, Elisabeth Badens

Sclareol Purification Using the Supercritical Fractionation Process: A Modeling Case Study

C. Dufour [a,b], C. Crampon [a,*], C. Delbecque [b], P-P. Garry [b], and E. Badens [a]

[a] Aix Marseille Univ, CNRS, Centrale Marseille, M2P2, Marseille, France

[b] Bontoux SAS; Quartier Aguzon – Le Clot 26170 Saint Auban sur l'Ouveze; France

* christelle.crampon@univ-amu.fr

Abstract

The aim of this study was to model experimental results obtained for the supercritical CO_2 fractionation of a liquid mixture containing 24% of sclareol in order to recover a raffinate with increased sclareol content. First, supercritical CO_2 fractionation experiments were carried out at pressures (10 to 12) MPa, and temperatures (313 to 338) K. Secondly, the modeling of the raffinate and extract compositions for 12 selected compounds including sclareol was performed using the group method. The modeling was carried out at a temperature of 323 K and pressures of (10 to 11) MPa, and at a temperature of 338 K and a pressure of 12 MPa. The calculation of the raffinate and extract compositions required the adjustment of the number of theoretical stages and of the distribution coefficients for the selected compounds. Experimental raffinate and extract compositions were represented by the model with a relative error of about 15%.

Keywords: Supercritical carbon dioxide; Fractionation; Counter-current column; Sclareol; Group method

1. Introduction

Clary sage (*Salvia sclarea* L.) is a very odorous herbaceous plant [1], endemic to Provence in the South of France. The calyx of Clary sage flowers contains about 1-4% of sclareol [2]

which is a raw material used in perfumery for the production of Ambrox® or Ambroxan® [3,4]. Sclareol (fig. 1) is used as a base and fixative note with a view to substituting natural ambergris (whale intestinal secretions).

The aim of this study was to carry out the modeling of experimental data obtained by fractionating a clary sage complex mixture containing 24% of sclareol and about 200 other compounds, using supercritical CO_2, with a simple method already applied to supercritical fractionation results [5].

Very little modeling of the supercritical fractionation process according to this approach is proposed in the litterature. Mathematical models do not often take into account the physical phenomena such as the model used by Varona *et al.* [6]. Other models, such as Martín and Cocero's, study the purification of one single compound [7]. To carry out this modeling, the choice fell upon a simple model called the group method, which was developped by Kremser [8] for absorbers and improved by Edminster [9] for vapor/liquid separations under low pressure. Henley and Seader [10] then applied this method to the vapor/liquid separation of hydrocarbons. More recently, Pieck *et al.* [5] used the group method to represent the supercritical fractionation of an esterified fish oil.

The supercritical fractionation is a process allowing the compounds contained in a liquid mixture to be separated by using a solvent under supercritical conditions. The feed diluent and the solvent must not be miscible under the implemented operating conditions. Supercritical fractionation process is generally carried out in continuous mode, using a counter-current packed column, in which the liquid feed and the supercritical solvent are introduced at the top and bottom of the column respectively, and put in contact with each other [11,12]. In this configuration, supercritical fractionation is similar to absorption where the extract (or light phase) composed of the most soluble compounds in the supercritical solvent is recovered at the top of the column. Conversely, the raffinate, corresponding to the highest density phase

containing the least soluble compounds, is collected at the bottom of the column. Carbon dioxide (CO_2) is the most frequently encountered solvent for the supercritical fractionation operation and allows such a process to cumulate many advantages when compared to conventional techniques. First of all, supercritical CO_2 fractionation is a sustainable and continuous process. The process selectivity can be tuned according to the pressure and temperature conditions applied in the column, which are directly linked to the physico-chemical properties of supercritical CO_2, and according to the feed and solvent flowrates on which the hydrodynamics depends. CO_2 can be easily recycled and the raffinate and the extracts are free of solvent since gaseous CO_2 is spontaneously separated after depressurization. A post-treatment is generally not required. Even if supercritical fractionation involves high pressure equipment, it can be economically viable thanks to its compacity and flexibility. In addition, it is a low temperature operation which allows processing thermolabile compounds. To conclude, supercritical CO_2 fractionation can be an interesting alternative for complex separations [13]. Finally, this operation can also be coupled with conventional ones to improve their overall separation efficiency.

In this work, an experimental study followed by a modeling stage is proposed. In the first step, experiments were conducted at pressures of (10 to 12) MPa, at temperatures of (313 to 338) K and for solvent-over-feed ratios between 13 and 173 with the objective of obtaining a sclareol-rich raffinate, the solubility of sclareol in supercritical CO_2 being low. These operating conditions were determined after a preliminary study presented in a previous article [14]. In the second step, the group method was used to model the distribution of sclareol and 11 selected compounds in extract and raffinate during the supercritical CO_2 fractionation process. The assumptions for the model application were checked and the number of theoretical stages and the distribution factors for each selected coumpound were adjusted on

experimental composition data. Finally, the calculated compositions in raffinate and extracts were compared to the experimental ones.

2. Materials and Methods

2.1. Materials

Carbon dioxide with a purity of 99.7% was supplied by Linde Gaz (France).

The studied feed used for supercritical CO_2 fractionation experiments was provided by the company Bontoux SAS (Saint Auban sur l'Ouvèze, France). This liquid mixture was the lightest fraction of an extract obtained from Clary sage flowers and was composed of 24 wt% of sclareol as well as about 200 other compounds.

2.2. Experimental set-up

Fig. 2 shows a simplified schematic diagram of the supercritical CO_2 fractionation apparatus. The apparatus and procedure have already been described in a previous paper [14]. The unit consists in a 2.6 m high packed column with a 30 mm internal diameter.

A typical run was carried out as follows: the column was first heated up to the targetted temperature before CO_2 was introduced. A CO_2 high-pressure piston pump was then set at the desired flow rate and operating pressure by means of a back-pressure regulator. When the steady-state was installed relative to CO_2, the liquid mixture was introduced at the desired flow rate using a piston pump. Extract and raffinate samples were collected and analyzed at regular time intervals and steady-state conditions were assumed to be reached as soon as the standard deviations for three successive samples were less than 1wt% of sclareol. After repeatability tests, the experimental raffinate and extract compositions were determined with an uncertainty around 2.6% and the error on the ratio S/Z (solvent massic flowrate divided by the liquid mixture massic flowrate) was about 3%.

Experimental data were obtained for operating conditions as follows: temperatures between 313 K and 338 K, pressures between 10 MPa and 12 MPa and for solvent-over-feed ratios between 13 and 173. These operating conditions were deduced after a preliminary study presented in a previous article [14]. The objective was to find the optimum operating conditions for concentrating sclareol in the raffinate.

2.3. Analytical methods

The process input (feed mixture) and outputs (extract and raffinate collected through the fractionation experiments) were analyzed by gas chromatography with a column HB5HT: 15 m × 0.25 mm × 0.1 µm with Flame Ionization Detector (FID) (Autosystem XL, Perkin Elmer). The recovered extract and the liquid feed mixture were diluted to 20% in chloroform (Sodipro, 99.5%). Diethyl phthalate (Grasse Chimie's World, 99.5%) was used as a standard for the quantification of sclareol.

2.4. Modeling

The extract and raffinate compositions were calculated using a model based on the group method developed by Kremser and Edmister [8] for the modeling absorption process. The choice fell on this model because it had already been validated on the experimental results of Pieck *et al.* [5].

The model is based on a simple relation linking the extraction yield (ε) and the stripping factor (ξ_i) for each component *i* (Eq. 1).

$$\xi_i = K_i \varepsilon \quad (1)$$

Where K_i is the overall distribution coefficient of component *i*, and ε, the extraction yield, is the ratio between the extract mass flow rate *E* and the feed mass flow rate *Z*. The extraction

yield ε is calculated as follows (Eq. 2), considering that the feed mass flowrate Z is equal to the sum of the extract mass flow rate E and the raffinate mass flow rate R:

$$\varepsilon = \frac{E}{Z} = \frac{E}{E+R} \quad (2)$$

The stripping loss was determined by (Eq. 3):

$$\varphi_{S.i} = \frac{(1-\varepsilon)(\xi_i - 1)}{\xi_i^n(\xi_i - \varepsilon) + (1-\varepsilon)} \quad (3)$$

The expression shown as eq. 3 can be used to compute the extract and raffinate compositions (respectively X^E and X^R) if the stripping loss for each component i is known.

$$X_i^E = \frac{(1-\varphi_{S.i})X_i^Z}{1-\varphi_{S.j}X_j^Z} \quad (4)$$

$$X_i^R = \frac{\varphi_{S.i}X_i^Z}{\varphi_{S.j}X_j^Z} \quad (5)$$

X_i^Z is the composition of compound i in the feed.

The error distribution in the experimental data was assumed to be log-normal. Hence, the number of theoretical stages n and the overall distribution ratio K_i were fitted altogether to experimental data using the GRG (Generalized Reduced Gradient) nonlinear Solving Method from the Microsoft Excel solver, by minimizing the objective function (Eq. 6):

$$f = \sum_{\forall i} \left(ln\left(X_i^{exp}\right) - ln\left(X_i^{calc}\right) \right)^2 \quad (6)$$

In which X_i represents both the extract and raffinate mass fractions of the selected components i and the rest of the compounds cumulated into a single pseudo-component.

Modeling using the group method requires the validation of two hypotheses: that the steady-state is established and the studied mixture is considered as ideal.

3. Results and discussion

3.1. Experimental results

For each experimental condition, the overall mass balance in sclareol was satisfactory since the mean deviation was 2%. For all experiments, the compound of interest, sclareol, was concentrated in the raffinate. Table 1 gives the experimental results obtained for the operating conditions studied.

Z, S, R, and *E*, are the mass flow rates of the feed, supercritical CO_2, raffinate, and extract, respectively. X^Z is the mass fraction of sclareol in the feed and X^R, and X^E, are the supercritical solvent-free mass fractions of sclareol in the raffinate and the extract, respectively. β^* is the ratio between the recalculated mass fraction of sclareol in the feed from a partial mass balance when the steady state was assumed, and the initial mass fraction in the feed. Finally, τ is the sclareol yield in the raffinate.

Figs. 3 to 5 regroup the results obtained and highlight the influence of pressure, temperature, and CO_2-over-feed ratio (*S/Z*) on the mass fraction of sclareol (a) in the extract and in the raffinate, and on the sclareol yield (b) in the raffinate.

Fig. 3 (a) illustrates the influence of temperature on the mass fraction of sclareol at a pressure set to 10 MPa, as a function of the CO_2-over-feed mass ratio. Assays were conducted at three temperatures 313 K, 323 K and 333 K. At a constant CO_2-over-feed ratio, a decrease in temperature led to an increase in the mass fraction of sclareol in the raffinate. However, a slight increase in the content of sclareol in the extract was also noted. This behavior appears clearly in Fig. 3 (b) which shows the evolution of the sclareol yield in the raffinate versus the ratio *R/(E+R)*. At 10 MPa, a decrease in the temperature thus led to a decrease in the selectivity. Experiments at 313 K were thus no longer conducted in order to avoid the sharing of sclareol between the raffinate and the extract. Moreover, at 313 K, it was not possible to work at a CO_2-over-feed mass ratio bigger than 40. Above this value, no raffinate was withdrawn, maybe due to a partial crystallization of the sclareol in the column.

Fig. 4 and 5 show the influence of pressure at two temperatures: 323 K and 338 K. Fig. 4 (a) highlights that a 338 K pressure had a slight influence on the mass fraction of sclareol in the extract, whatever the CO_2-over-feed ratio from 15 up to 160. The influence of pressure was a little more pronounced on the sclareol content in the raffinate since at a constant CO_2-over-feed ratio, the mass fraction of sclareol at 12 MPa is slighly higher than at both 10 MPa and 11 MPa. Even in Fig. 4 (b) which illustrates the evolution of the sclareol yield versus the ratio *R/(R+E)*, no significant influence of pressure was noted.

Some assays were finally carried out at 323 K (Fig. 5). At that temperature, the pressure had a significant influence on the mass fraction of sclareol both in the raffinate and the extract. At the highest pressure of 12 MPa, Fig. 5 (b) reveals the fall in sclareol yield while the ratio *R/(R+E)* decreased. As for the temperature of 313 K, at 323 K there was a drop in the selectivity when the pressure increased.

3.2 Selection of the 12 compounds from the feed selected for modeling

The liquid mixture to be fractionated was composed of about 200 different compounds. In this work, 12 compounds including sclareol were selected to study their distribution in the extract and in the raffinate versus the extraction yield. The choice fell on compounds easily identifiable by gas chromatography, distributed over the entire length of the chromatogram, having interesting behavior for sclareol purification, and present both in the extract and the raffinate. Sclareol (I_{12}), together with seven major compounds (named I_1 to I_7) were identified as major compounds in the mixture. Four impurities (named I_8 to I_{11}) characterized the quality of the separation since they are due to the degradation of sclareol during storage and prove difficult to remove by currently used purification techniques. Fig. 6 shows the gas chromatographic profile of the feed in which the selected compounds are highlighted and table 2 gives the content of the selected compounds in the feed.

3.3. Assumptions for model application

The first assumption to be checked is that the steady-state was well established. To that aim, the mass balance for each component *i* in the feed should be verified:

$$Z_i = E_i + R_i \quad (5)$$

With Z_i, E_i and R_i the massic flow rates of compound i in the feed, extract and raffinate, respectively.

The following equation is obtained:

$$X_i^Z = X_i^E \varepsilon + X_i^R (1 - \varepsilon) \quad (7)$$

The right term represents the global composition of the X_i^Z feed calculated using the mass fraction measured in the extract X_i^E and in the raffinate X_i^R. This calculated value has to be compared to the experimental one. If the mass balance is verified, when plotting the calculated mass fraction in the feed versus the experimental corresponding value, a straight line passing through the origin and with a slope of 1 is obtained. Fig. 7 shows the calculated $(X_i^Z)_{calc}$ versus the experimental $(X_i^Z)_{exp}$ and thus illustrates the mass balance obtained for the selected components at 10 MPa and 323 K. As a proportionality is observed between the calculated and the experimental mass fractions, with in addition a slope of the straight line very close to 1, the steady-state was well established.

The second assumption to be checked for the application of the model is that the studied mixture can be considered as an ideal mixture, meaning that the solubility of each compound in CO_2 is independent of the proportion of each compound in the mixture. If the solubility is considered independent of the composition, the extraction yield is a linear function of the solvent-over-feed ratio (S/Z). This hypothesis was checked for three studied operating conditions: a temperature of 323 K for pressures of 10 MPa and 11 MPa and a temperature of

338 K for a pressure of 12 MPa. Fig. 8 shows the extraction yield versus the CO_2-over-feed ratio for experiments carried out at 323 K and 10 MPa. A straight line of equation ($y = 0.004\ x$) was obtained leading to the conclusion that the feed mixture could be considered as ideal under such operating conditions.

3.4. Modeling of the extract and raffinate compositions

The model was applied for three different operating conditions that respected the assumptions of the model (323 K for pressures of 10 MPa and 11 MPa and 338 K for a pressure of 12 MPa) and table 3 gives the estimation of overall distribution coefficient (K_i) for each compound and each operating condition. Fig. 9 shows the modeling of the 12 compounds selected in the mixture.

The estimation of the distribution coefficients in table 3 and the curves obtained in Fig. 9 emphasize three different types of behavior. Firstly, compounds I1, I2, I3, I4 and I6 behaved similarly (Fig. 9 (a-d) and (e)). Indeed, they had a distribution coefficient greater than 1 so that they were preferentially collected in the extract. On the contrary, compounds I7, I8, I9, I10, I11, and the sclareol had a distribution coefficient lower than 1; they were indeed collected in the raffinate (Fig. 9 (f-l)). And finally, a third type of behavior was observed: compound I5 had a distribution coefficient around 1 and was evenly distributed between the extract and the raffinate (Fig. 9 (e)).

Experimental data were represented by the model with a relative error of about 15% which is satisfactory regarding the complexity of the system. Indeed, it was a natural extract with a real industrial application. The same error of 15% was determined by Pieck *et al.* [5]. Varona *et al.* [6] predicted the separation factor with an average deviation of 20%. Fig. 10 compares the experimental composition values to the calculated ones for the three operating conditions considered and for the 12 selected compounds. A good correlation was observed between the

model and the experimental data. The points outside the outline were those corresponding to traces of the light compounds in the raffinate, implying a bigger error between the model and the experimental data.

4. Conclusion

Supercritical CO_2 fractionation was applied to a complex feed mixture containing more than 200 compounds with the objective of concentrating sclareol in the raffinate. The group method was used in order to model the compositions of 12 selected compounds including sclareol. Although such a model may only suit ideal mixtures, a good correlation was obtained between experimental compositions and calculated values for three different operating conditions. A relative error of about 15% was reached and for such a complex system, those results can be considered as satisfactory. Moreover, modeling allowed to highlight three different types of behavior in relation to the values of the distribution coefficients. Compounds having a distribution coefficient greater than 1 were preferentially collected in the extract; when the distribution coefficients were lower than 1, the compounds were collected in the raffinate; and, finally, the compounds fairly distributed between the extract and the raffinate had distribution coefficients close to 1. Such modeling, although its simplicity, may offer a better understanding of component behavior when considering the separation of complex mixtures using supercritical fractionation.

References

[1] D.C. Hao, S.L. Chen, A. Osbourn, V.G. Kontogianni, L.W. Liu, M.J. Jordán, Temporal transcriptome changes induced by methyl jasmonate in Salvia sclarea, Gene 558 (2015) 41-53. http://dx.doi.org/10.1016/j.gene.2014.12.043.

[2] J.C. Caissard, T. Olivier, C. Delbecque, S. Palle, P-P. Garry, A. Audran, N. Valot, S. Moja, F. Nicolè, J-L. Magnard, S. Legrand, S. Baudino, F. Jullien, Extracellular Localization of the Diterpene Sclareol in Clary Sage (Salvia sclarea L., Lamiaceae), PLoS ONE 7 (2012) e48253. https://doi.org/10.1371/journal.pone.0048253.

[3] A. Caniard, P. Zerbe, S. Legrand, A. Cohade, N. Valot, J-L. Magnard, J. Bohlmann, L. Legendre, Discovery and functional characterization of two diterpene synthases for sclareol biosynthesis in Salvia sclarea (L.) and their relevance for perfume manufacture, BMC Plant Biol. 12 (2012) 119-132. https://doi.org/10.1186/1471-2229-12-119.

[4] C. Schmiderer, P. Grassi, J. Novak, M. Weber, C. Franz, Diversity of essential oil glands of clary sage (Salvia sclarea L., Lamiaceae), Plant Biol. 10 (2008) 433‑440. https://doi.org/10.1111/j.1438-8677.2008.00053.x

[5] C.A. Pieck, C. Crampon, F. Charton, E. Badens, A new model for the fractionation of fish oil FAEE, J. Supercrit. Fluids 120 (2017) 258-265. http://dx.doi.org/10.1016/j.supflu.2016.05.024.

[6] S. Varona, A. Martín, M.J. Cocero, T. Gamse, Supercritical carbon dioxide fractionation of Lavandin essential oil: Experiments and modeling, J. Supercrit. Fluids 45 (2008) 181‑188. https://doi.org/10.1016/j.supflu.2007.07.010.

[7] A. Martín and M.J. Cocero, Mathematical modeling of the fractionation of liquids with supercritical CO_2 in a countercurrent packed column, J. Supercrit. Fluids 39 (2007) 304‑314. https://doi.org/10.1016/j.supflu.2006.03.004.

[8] A. Kremser, Theoretical analysis of absorption columns, Nat. Petroleum News, 22 (1930), 43-49.

289 [9] W.C. Edmister, Absorption and stripping-factor functions for distillation calculation by
290 manual- and digital-computer methods, AIChE J. 3 (1957), 165-171.
291 https://doi.org/10.1002/aic.690030207.
292 [10] E. Henley and J. Seader, Approximate Methods for Multicomponent, Multistage
293 Separations, in: Equilibrium-stage separation operations in chemical engineering. Wiley,
294 1981, pp. 427-500.
295 [11] G. Brunner, Counter-current separations, J. Supercrit. Fluids 47 (2009) 574-582.
296 https://doi.org/10.1016/j.supflu.2008.09.022.
297 [12] A. Bejarano, P.C. Simões, J.M. del Valle, Fractionation technologies for liquid mixtures
298 using dense carbon dioxide, J. Supercrit. Fluids 107 (2016) 321-348.
299 http://dx.doi.org/10.1016/j.supflu.2015.09.021.
300 [13] C.A. Pieck, C. Crampon, F. Charton, E. Badens, Multi-scale experimental study and
301 modeling of the supercritical fractionation process, J. Supercrit. Fluids 105 (2015), 158-169.
302 http://dx.doi.org/10.1016/j.supflu.2015.01.021.
303 [14] C. Dufour, C. Crampon, C. Delbecque, P.-P. Garry, E. Badens, Purification of sclareol by
304 supercritical CO_2 fractionation process, J. Supercrit. Fluids 122 (2017) 35-42.
305 http://dx.doi.org/10.1016/j.supflu.2016.12.001.

306

307

Figure captions

Fig. 1. Sclareol skeletal formula.

Fig. 2. Supercritical fluid fractionation unit.

Fig. 3. Evolution of the mass fraction of sclareol (a) in the extract at 313 K (○), 323 K (Δ), and 338 K (□) and in the raffinate at 313 K (●), 323 K (▲), and 338 K (■) versus CO_2-over-feed ratio (*S/Z*) when pressure is set to 10 MPa; evolution of the yield in sclareol (b) in the raffinate versus the ratio *R/(R+E)* at 10 MPa and for temperatures of 313 K (●), 323 K (▲), and 338 K (■).

Fig. 4. Evolution of the mass fraction of sclareol (a) in the extract at 10 MPa (○), 11 MPa (□), and 12 MPa (Δ) and in the raffinate at 10 MPa (●), 11 MPa (■), and 12 MPa (▲) versus CO_2-over-feed ratio (*S/Z*) when temperature is set to 338 K; evolution of the yield in sclareol (b) in the raffinate versus the ratio *R/(R+E)* at 338 K and for pressures of 10 MPa (●), 11 MPa (■), and 12 MPa (▲).

Fig. 5. Evolution of the mass fraction of sclareol (a) in the extract at 10 MPa (○), 11 MPa (□), and 12 MPa (Δ) and in the raffinate at 10 MPa (●), 11 MPa (■), and 12 MPa (▲) versus CO_2-over-feed ratio (*S/Z*) when temperature is set to 323 K; evolution of the yield in sclareol (b) in the raffinate versus the ratio *R/(R+E)* at 323 K and for pressures of 10 MPa (●), 11 MPa (■), and 12 MPa (▲).

Fig. 6. Chromatographic profile of the feed containing about 24% of sclareol with an identification of the 12 selected compounds. Refer to Table 3 for peak identification.

Fig. 7. Mass balance checking for the essays performed at 10 MPa and 323 K – Calculated global fraction in the feed $(X_i^Z)_{calc}$ versus the experimental one $(X_i^Z)_{exp}$. The slope of the straight line is equal to 1.0081 and the regression parameter is equal to 0.9962.

Fig. 8. Extraction yield versus the CO_2-over-feed ratio at 323 K and 10 MPa – the slope of the straight line is equal to 0.004 and the regression coefficient R^2 is equal to 0.9761.

Fig. 9. Evolution of the raffinate and extract composition of I1 (a), I2 (b), I3 (c), I4 (d), I5 (e), I6 (f), I7 (g), I8 (h), I9 (i), I10 (j), I11 (k), and sclareol (l) versus extract yield for a fractionation performed under 10 MPa and a temperature of 323 K. Model output is represented by dashed (extract) and full (raffinate) lines. Squares represent experimental raffinate and circles represent experimental extract.

Fig. 10. Comparison between experimental and calculated compositions in the extract and the raffinate - Operating conditions: 323 K for pressures of 10 MPa and 11 MPa, and 338 K for a pressure of 12 MPa.

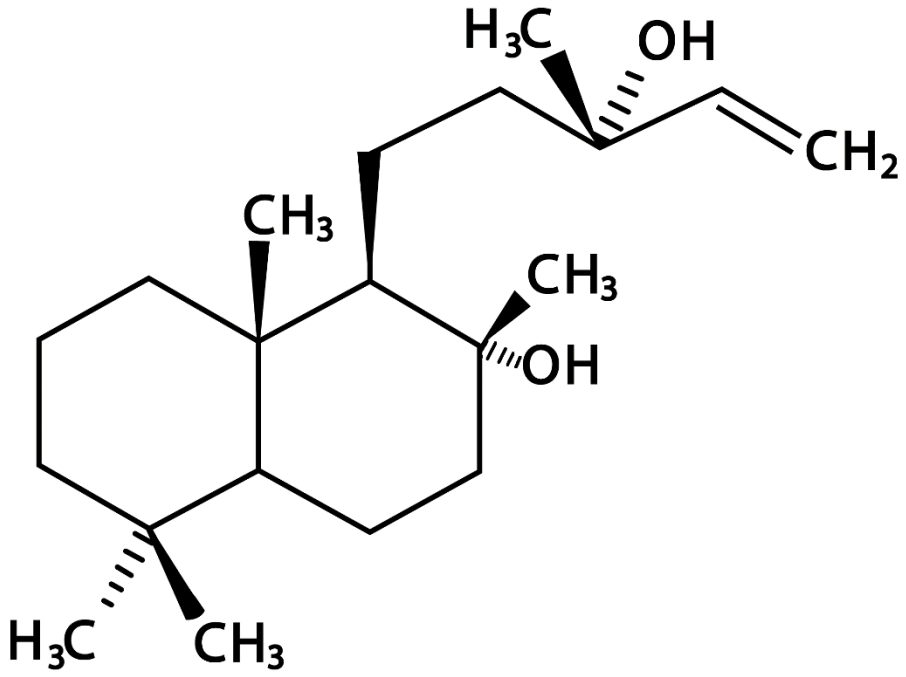

Fig. 1. Sclareol skeletal formula

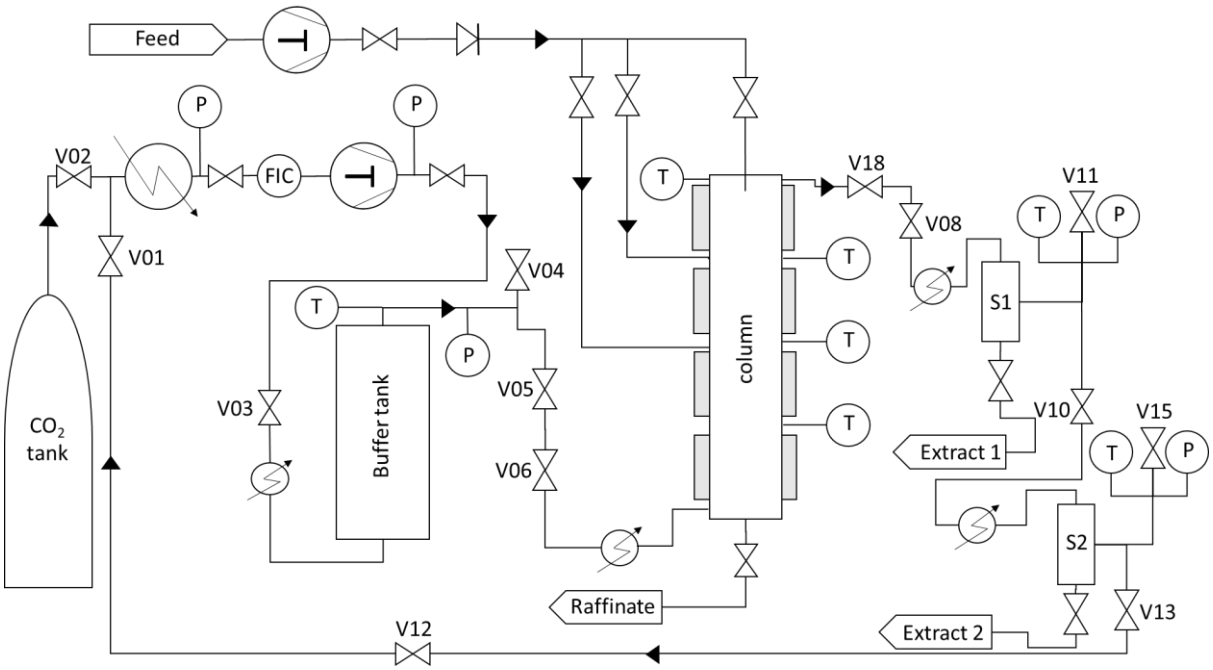

Fig. 2. Supercritical fluid fractionation set-up

V01 to V18 are valves; S1 and S2 are separators; T, P are temperature and pressure sensors

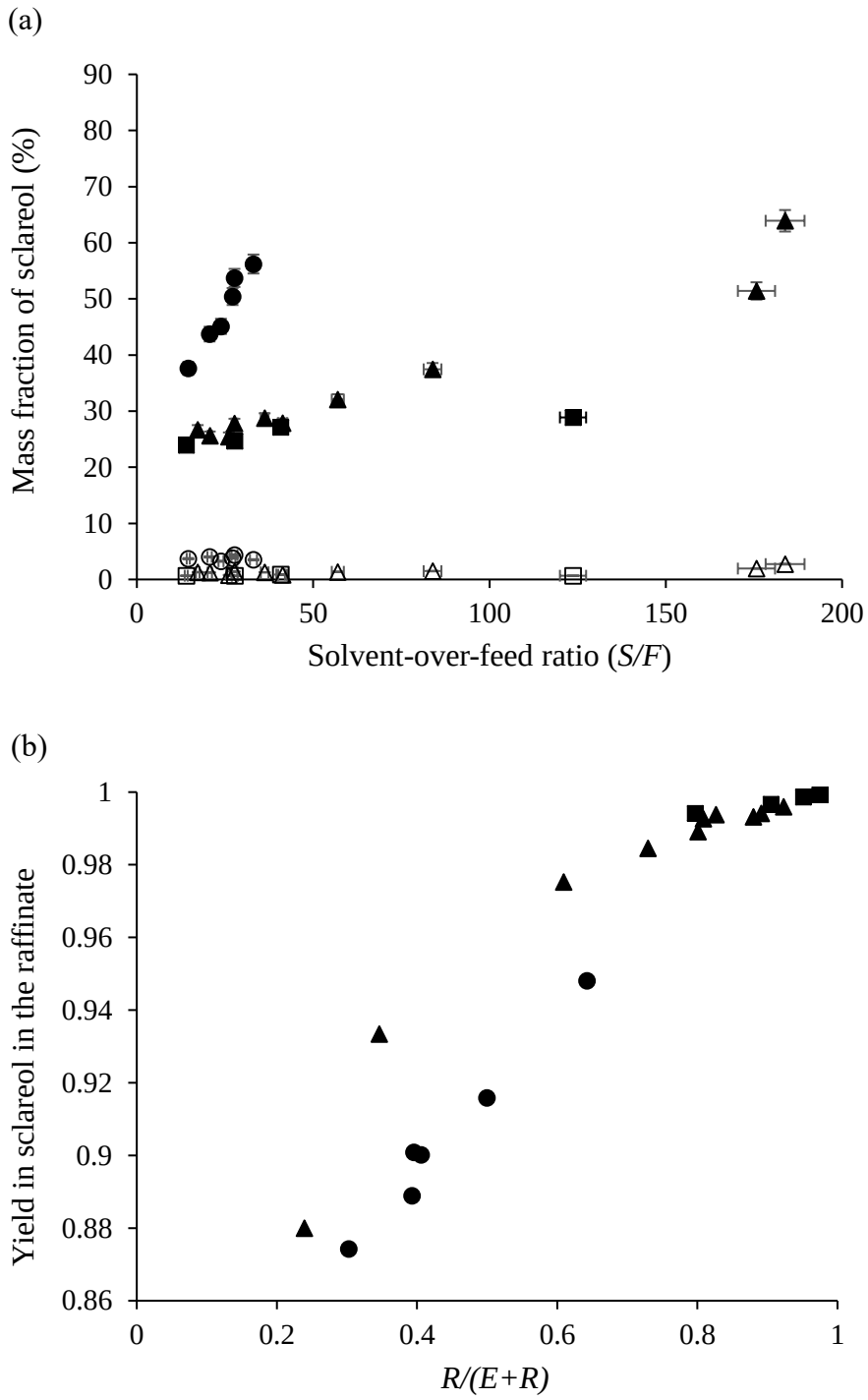

Fig. 3. Evolution of the mass fraction of sclareol (a) in the extract at 313 K (○), 323 K (∆), and 338 K (□) and in the raffinate at 313 K (●), 323 K (▲), and 338 K (■) versus CO_2-over-feed ratio (*S/Z*) when pressure is set to 10 MPa; evolution of the yield in sclareol (b) in the raffinate versus the ratio *R/(R+E)* at 10 MPa and for temperatures of 313 K (●), 323 K (▲), and 338 K (■).

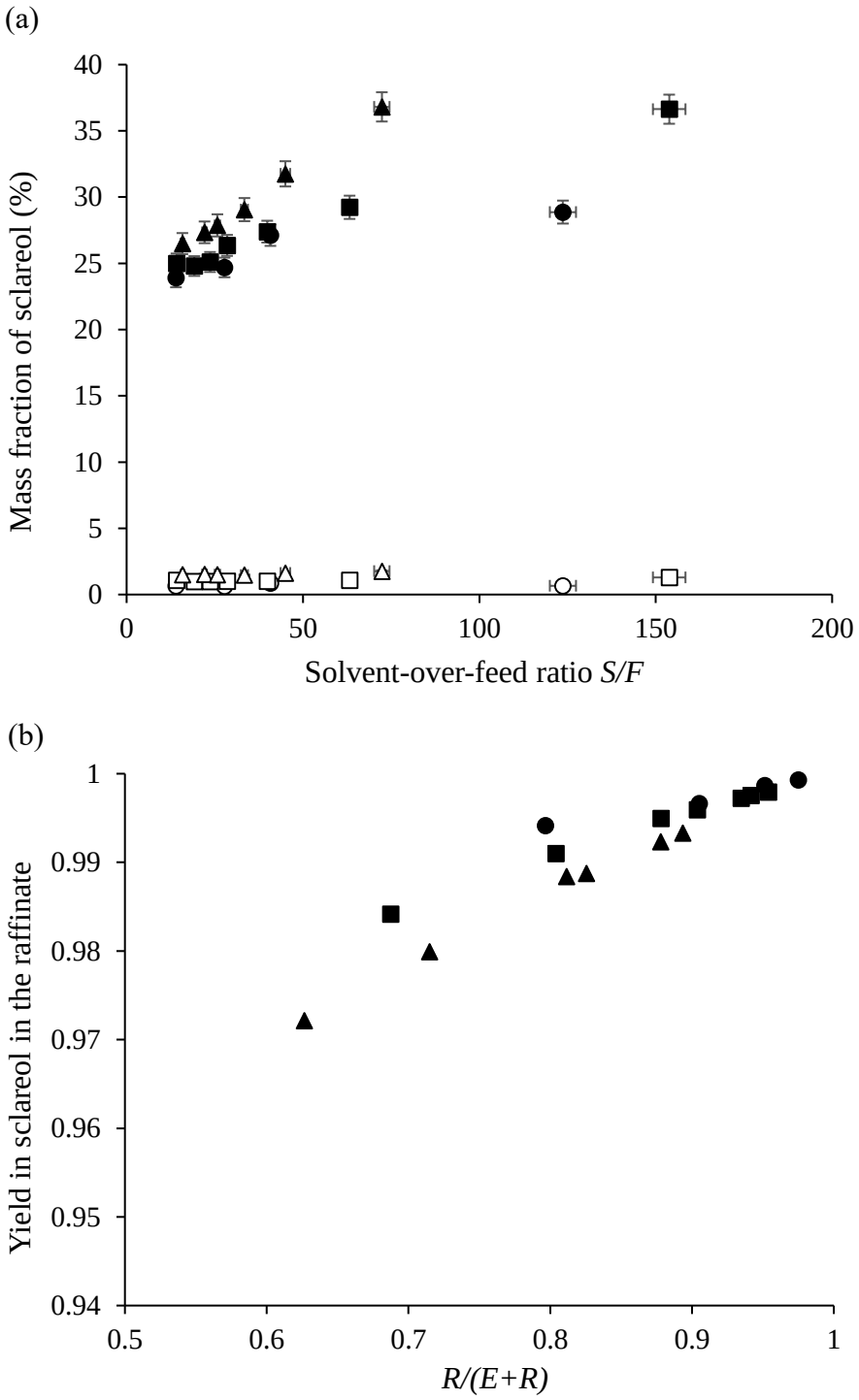

Fig. 4. Evolution of the mass fraction of sclareol (a) in the extract at 10 MPa (○), 11 MPa (□), and 12 MPa (Δ) and in the raffinate at 10 MPa (●), 11 MPa (■), and 12 MPa (▲) versus CO_2-over-feed ratio (*S/Z*) when temperature is set to 338 K; evolution of the yield in sclareol (b) in the raffinate versus the ratio *R/(R+E)* at 338 K and for pressures of 10 MPa (●), 11 MPa (■), and 12 MPa (▲).

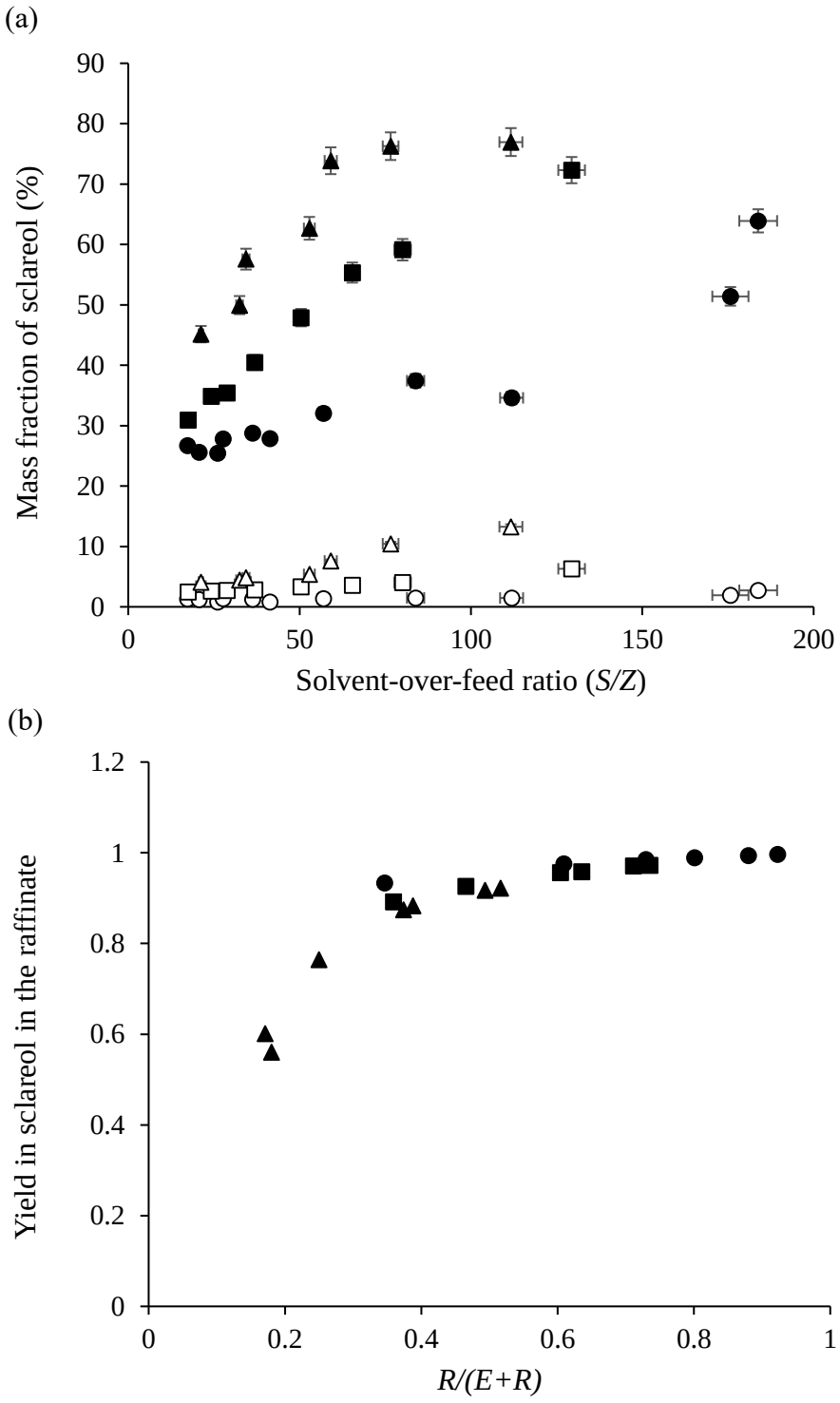

Fig. 5. Evolution of the mass fraction of sclareol (a) in the extract at 10 MPa (○), 11 MPa (□), and 12 MPa (Δ) and in the raffinate at 10 MPa (●), 11 MPa (■), and 12 MPa (▲) versus CO_2-over-feed ratio (*S/Z*) when temperature is set to 323 K; evolution of the yield in sclareol (b) in the raffinate versus the ratio *R/(R+E)* at 323 K and for pressures of 10 MPa (●), 11 MPa (■), and 12 MPa (▲).

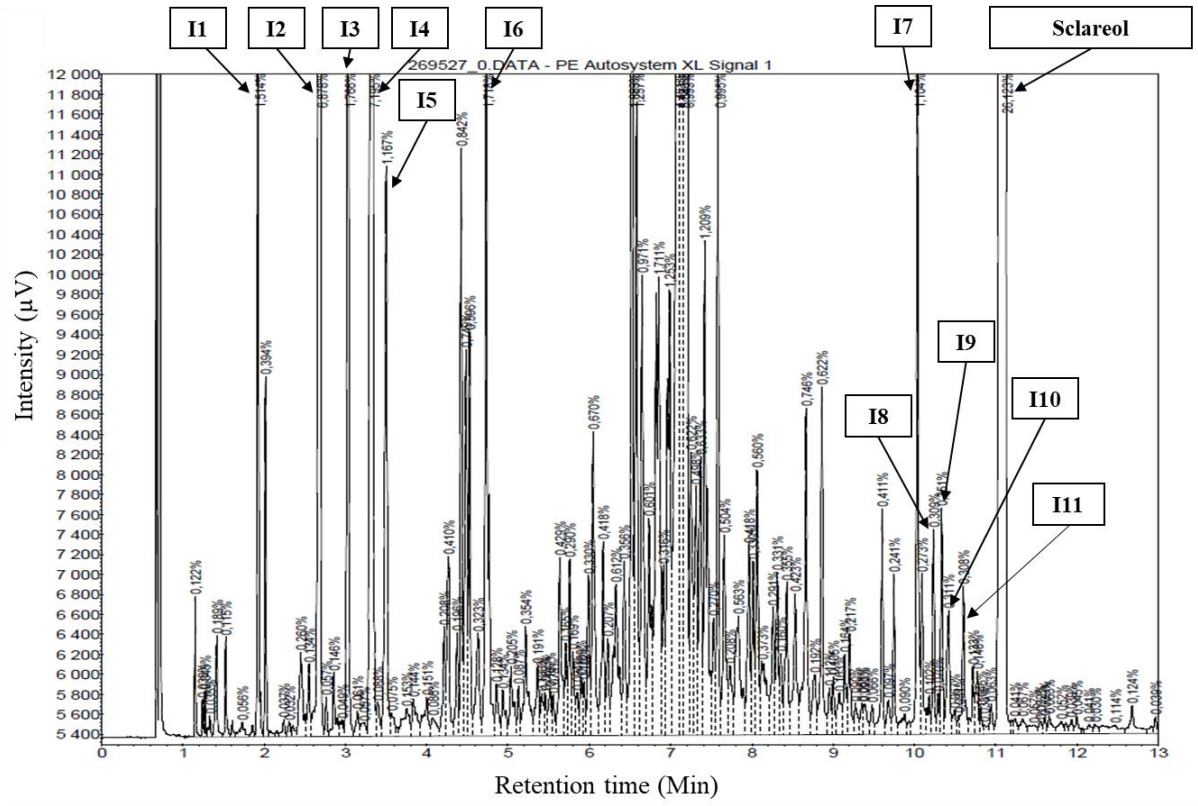

Fig. 6. Chromatographic profile of the feed containing about 24% of sclareol with an identification of the 12 selected compounds. Refer to Table 3 for peak identification.

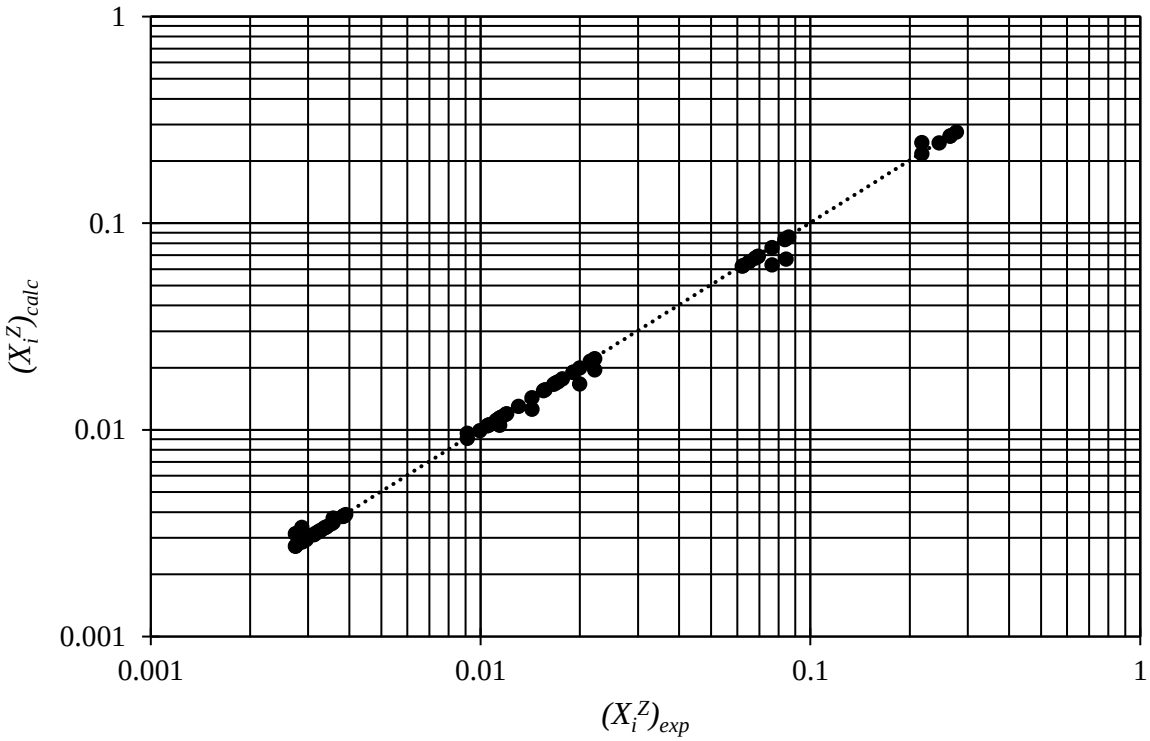

Fig. 7. Mass balance checking for the essays performed at 10 MPa and 323 K – Calculated global fraction in the feed $(X_i^Z)_{calc}$ versus the experimental one $(X_i^Z)_{exp}$. The slope of the straight line is equal to 1.0081 and the regression parameter is equal to 0.9962.

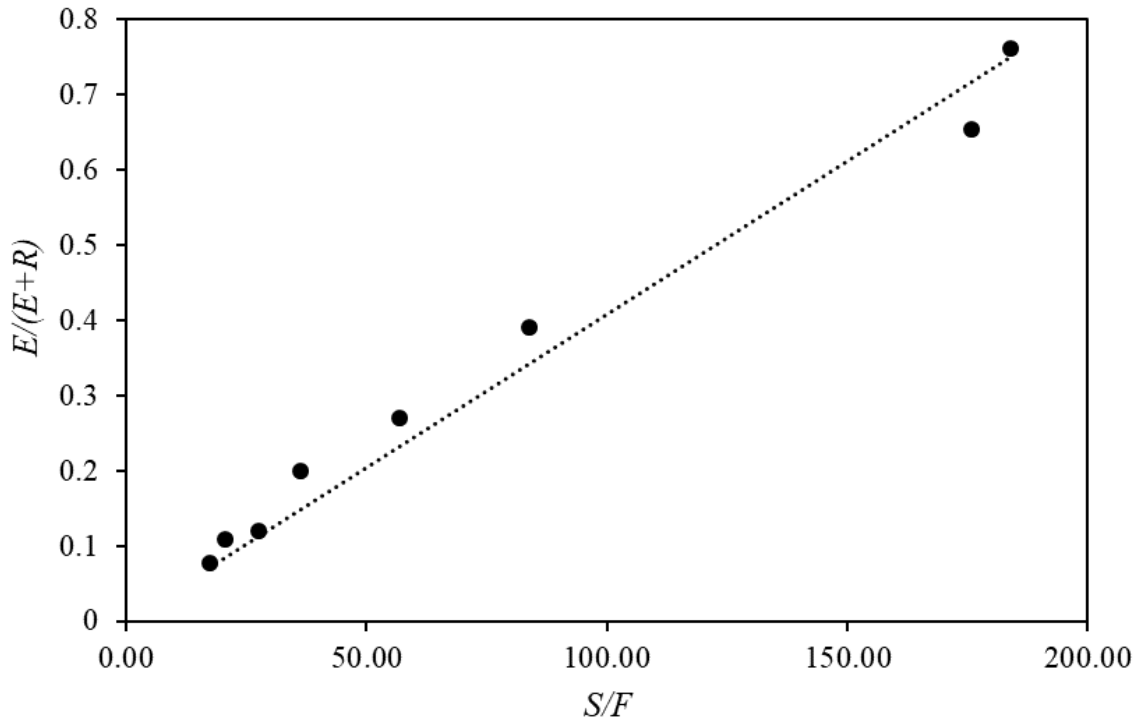

Fig. 8. Extraction yield versus the CO_2-over-feed ratio at 323 K and 10 MPa – the slope of the straight line is equal to 0.004 and the regression coefficient R^2 is equal to 0.9761

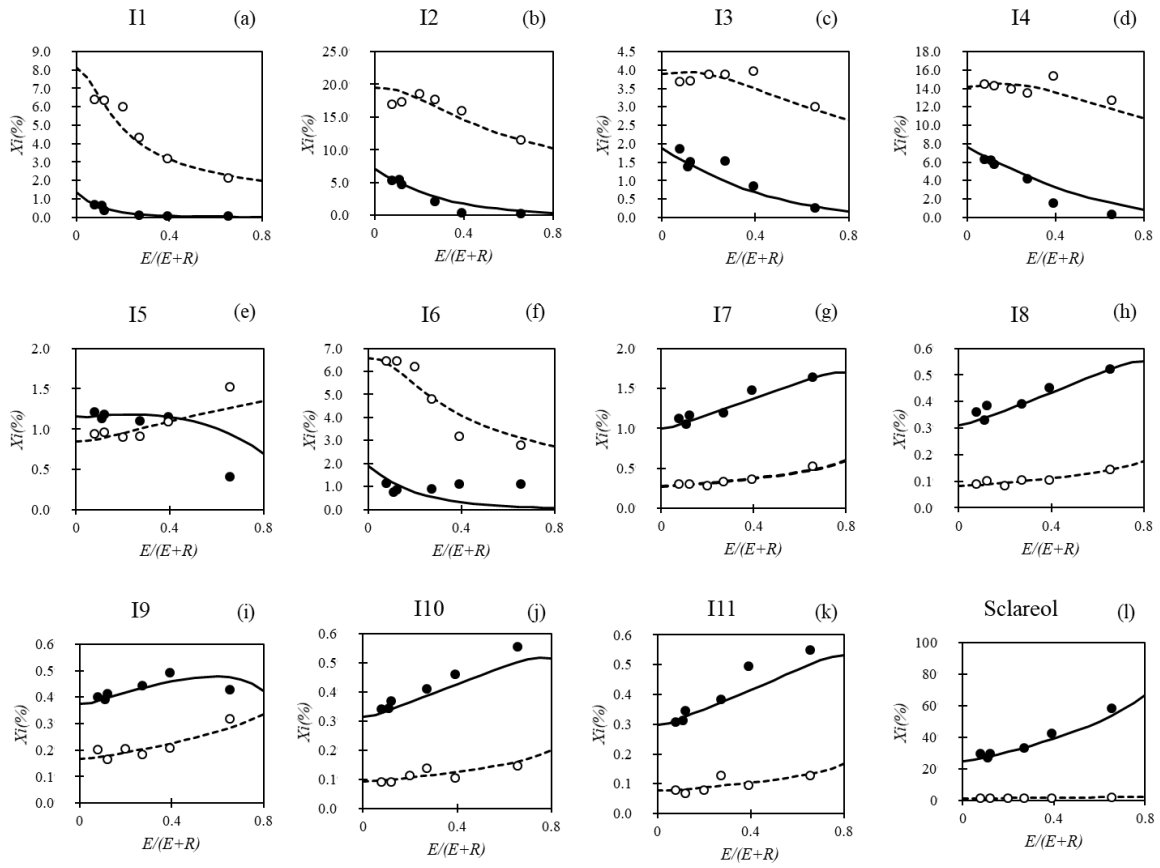

Fig. 9. Evolution of the raffinate and extract composition of I1 (a), I2 (b), I3 (c), I4 (d), I5 (e), I6 (f), I7 (g), I8 (h), I9 (i), I10 (j), I11 (k), and sclareol (l) versus extract yield for a fractionation performed under 10 MPa and a temperature of 323 K. Model output is represented by dashed (extract) and full (raffinate) lines. Squares represent experimental raffinate and circles represent experimental extract.

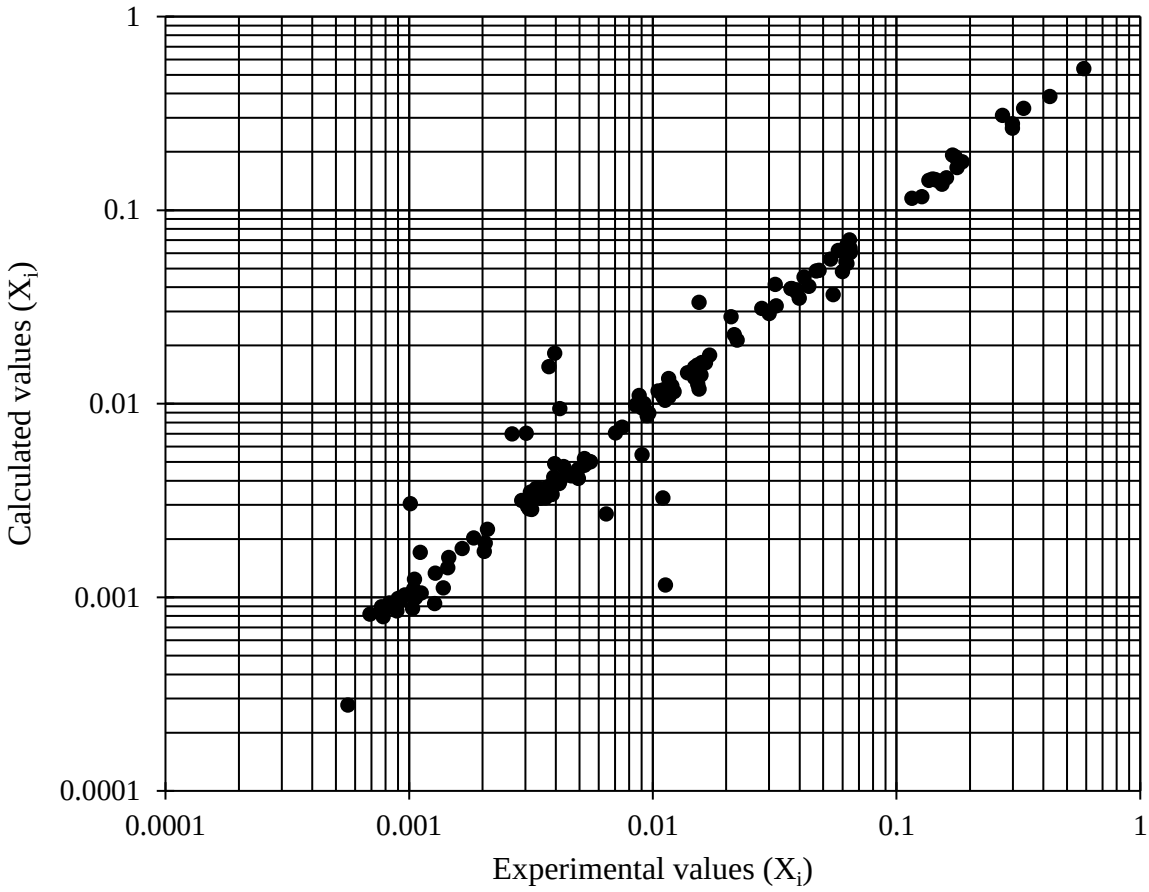

Fig. 10. Comparison between experimental and calculated compositions in the extract and the raffinate - Operating conditions: 323 K for pressures of 10 MPa and 11 MPa, and 338 K for a pressure of 12 MPa.

List of tables

Table 1. Experimental results obtained for operating conditions studied. *Supercritical solvent free mass fractions; **β: partial mass balance in sclareol

P (MPa)	T (K)	S (kg·h^{-1})	Z (kg·h^{-1})	X_Z ±0.1 (%)	E (kg·h^{-1})	X_E^* ±0.1 (%)	R (kg·h^{-1})	X_R^* ±0.1 (%)	β^{**}	τ (%)
10	338	27	1.93	23.3	0.049	0.7	1.88	23.9	0.99	99.9
		27	0.22	23.3	0.044	0.7	0.17	28.9	0.96	99.4
		27	0.97	23.3	0.048	0.6	0.93	24.7	1	99.8
		20	0.49	24.3	0.047	0.9	0.44	27.1	1	99.7
		40	1.43	24.0	0.26	1.6	1.17	27.6	0.95	98.7
		40	0.68	24.0	0.23	1.7	0.44	35.6	0.98	97.5
	323	20	1.16	24.5	0.089	1.3	1.07	26.7	1	99.6
		20	0.72	24.1	0.087	1.4	0.64	27.8	1	99.3
		20	0.55	22.7	0.11	1.3	0.44	28.8	1	98.9
		40	0.70	23.3	0.19	1.4	0.51	32.0	1	98.4
		40	0.48	21.4	0.19	1.5	0.29	37.4	1	97.5
		40	0.23	21.4	0.15	1.9	0.079	51.4	0.88	93.3
	313	20	1.37	24.5	0.49	3.7	0.88	37.6	1	94.8
		20	0.56	24.5	0.27	4.1	0.28	49.9	1	92.5
		40	1.94	24.3	0.97	4.0	0.97	43.7	0.98	91.6
		40	1.44	21.7	0.88	4.3	0.57	53.7	1	88.9
		40	1.47	22.0	0.87	3.8	0.60	50.4	1	90.0
		40	1.68	19.5	1.01	3.2	0.66	45.1	1	90.0
		40	1.17	19.5	0.69	3.6	0.47	49.8	1	90.6
		40	1.21	18.1	0.84	3.5	0.37	56.2	1	87.4
11	338	27	1.91	23.9	0.088	1.1	1.82	25.0	0.99	99.8
		27	1.41	23.9	0.082	1.0	1.32	24.8	0.97	99.8
		27	1.14	23.9	0.075	1.0	1.07	25.1	0.99	99.7
		27	0.95	23.9	0.091	1.0	0.86	26.4	1	99.6
		27	0.68	23.9	0.083	1.0	0.59	27.4	0.99	99.5
		27	0.43	23.8	0.083	1.1	0.34	29.2	0.98	99.1
		27	0.18	23.8	0.055	1.3	0.12	36.6	1	98.4
	323	34	1.94	24.6	0.51	2.5	1.43	30.9	0.95	97.2
		34	1.41	24.6	0.41	2.6	1.00	34.9	1	97.0
		34	1.18	24.4	0.43	2.7	0.75	35.4	0.96	95.8
		34	1.41	24.6	0.41	2.6	1.00	34.9	1	97.0
		34	1.18	24.4	0.43	2.7	0.75	35.4	0.96	95.8
		34	0.92	24.4	0.36	2.8	0.56	40.5	1	95.6
		34	0.67	24.4	0.36	3.3	0.31	47.9	0.98	92.6
		34	0.42	24.4	0.27	4.0	0.15	59.1	0.97	89.1
12	338	30	1.89	24.6	0.20	1.5	1.69	26.5	0.97	99.3
		30	1.36	24.6	0.17	1.5	1.19	27.3	0.98	99.2
		30	1.16	23.1	0.20	1.5	0.96	27.9	1	98.9
		30	0.90	23.1	0.17	1.5	0.73	29.1	1	98.8
		30	0.67	23.2	0.19	1.6	0.48	31.8	1	97.9
		30	0.41	23.2	0.15	1.7	0.26	36.8	1	97.2
	323	40	1.89	23.7	0.91	4.1	0.97	45.2	1	92.1
		40	1.23	23.7	0.62	4.4	0.61	49.9	1	91.7
		40	1.16	29.8	0.71	4.8	0.45	57.6	0.88	88.3
		40	0.76	29.8	0.47	5.4	0.28	62.7	0.89	87.4
		40	0.68	24.1	0.51	7.6	0.17	73.9	1	76.4
		40	0.36	24.1	0.29	13.3	0.065	76.9	1	56.0
		40	0.52	23.5	0.43	10.5	0.089	76.3	0.93	60.1

Table 2: Compounds selected for the modeling and their respective compositions in the feed - NI = Not Identified

Reference code	Name of selected compound	Overall estimated mass fraction in the feed (%)
I_1	Linalool	1.36
I_2	Alpha terpineol	7.14
I_3	Nerol	1.87
I_4	Linalyl acetate + geraniol	7.64
I_5	NI	1.16
I_6	NI	1.89
I_7	NI	0.99
I_8	NI	0.31
I_9	NI	0.37
I_{10}	NI	0.31
I_{11}	NI	0.29
Sclareol	Sclareol	24.2

Table 3. Distribution coefficients K_i and number of theoretical stages n obtained for each operating conditions

	Distribution coefficients K_i		
Reference code	**10 MPa - 323 K n = 2.2**	**11 MPa - 323 K n = 1.6**	**12 MPa - 338 K n = 4.1**
I_1	8.02	7.78	5.99
I_2	3.67	5.06	2.90
I_3	2.81	3.49	2.32
I_4	2.49	2.76	2.15
I_5	0.98	1.01	0.97
I_6	4.68	3.02	3.56
I_7	0.37	0.48	0.31
I_8	0.36	0.44	0.28
I_9	0.60	0.78	0.40
I_{10}	0.39	0.45	0.30
I_{11}	0.35	0.44	0.28
Sclareol	0.07	0.10	0.07

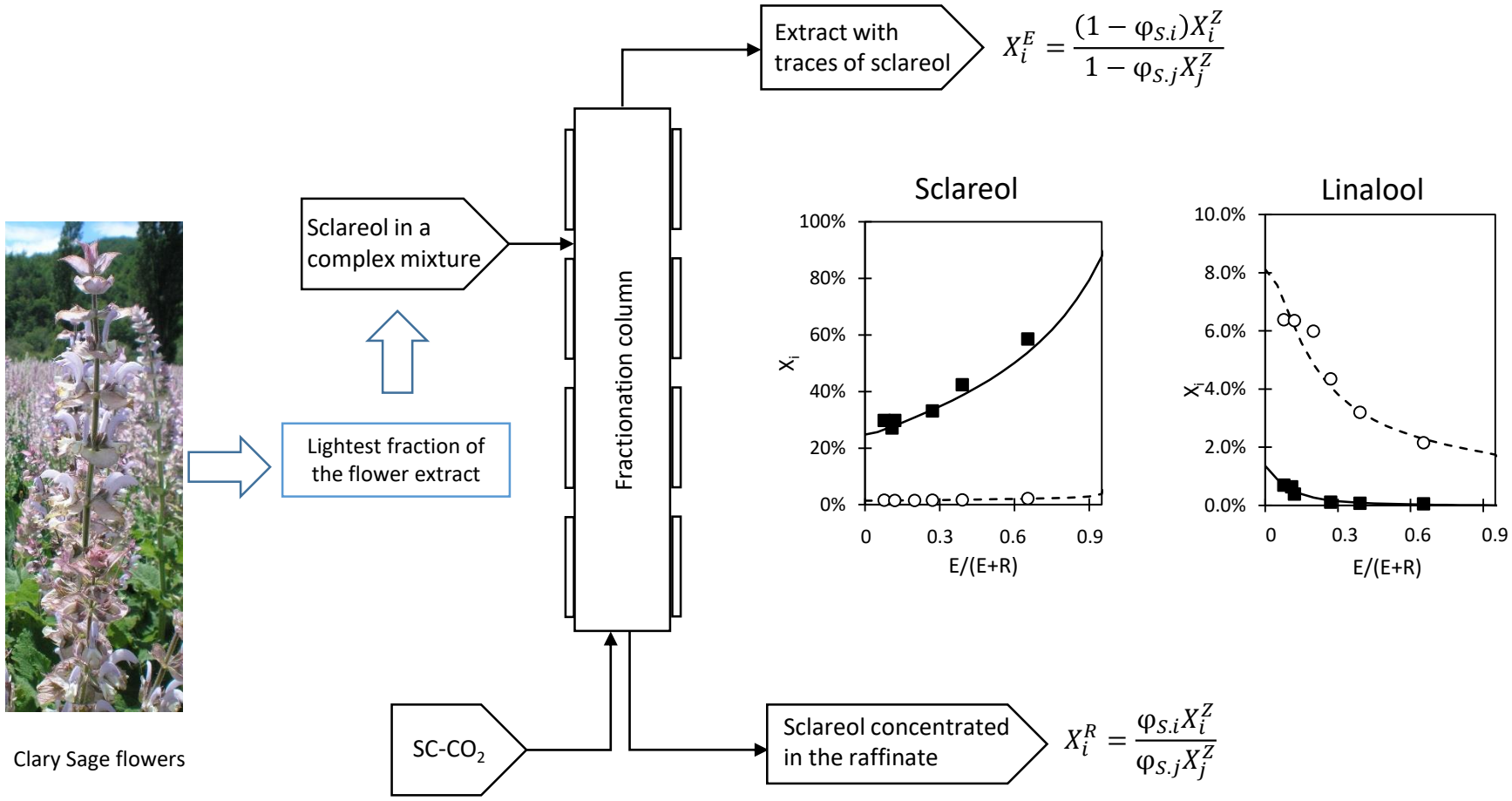
Extract with traces of sclareol
$X_i^E = \frac{(1-\varphi_{S.i})X_i^Z}{1-\varphi_{S.j}X_j^Z}$
Sclareol in a complex mixture
Lightest fraction of the flower extract
Fractionation column
SC-CO2
Sclareol concentrated in the raffinate
$X_i^R = \frac{\varphi_{S.i}X_i^Z}{\varphi_{S.j}X_j^Z}$
Sclareol
Linalool
100%
80%
60%
40%
20%
0%
10.0%
8.0%
6.0%
4.0%
2.0%
0.0%
0
0.3
0.6
0.9
E/(E+R)
Clary Sage flowers